JOURNAL OF CATALYSIS **160,** 43–51 (1996)
ARTICLE NO. 0122

Characterization of La^{3+}-Promoted Co/SiO_2 Catalysts

George J. Haddad, Bin Chen, and James G. Goodwin, Jr.[1]

Department of Chemical and Petroleum Engineering, University of Pittsburgh, Pittsburgh, Pennsylvania 15261

Received December 22, 1994; revised December 14, 1995; accepted January 19, 1996

In order to assess the distribution and the promotional effects of La^{3+}, a characterization study has been performed on a series of La^{3+}-promoted 20 wt% Co/SiO_2 catalysts of varying La/Co atomic ratios (0, 0.05, 0.1, 0.2, 0.3, 0.5, and 0.75) prepared by impregnation of prereduced and passivated Co/SiO_2 in order to minimize effects of promotion on Co particle size distribution. La^{3+} was found to be well dispersed over the Co/SiO_2 catalyst. However, it did not appear to be evenly distributed on the Co metal surface. From temperature programmed reduction, low La^{3+} loadings (La/Co $\leq$ 0.2) were found to moderate the strong Co–support interactions resulting from aqueous impregnation of Co/SiO_2 and to improve the reducibility of the Co oxide. [Aqueous impregnation of prereduced Co/SiO_2 has been shown earlier to result in the formation of Co silicates (Haddad, G. J., and Goodwin, J. G., Jr., *J. Catal.* 157, 25 (1995))]. On the other hand, high La^{3+} loadings (La/Co $\geq$ 0.5) appeared to induce La–Co compound and/or nonreducible Co-silicate formation, possibly due to the higher pH of the impregnating solution. The results indicate the multiple effects that promoters may have on supported metal catalysts. In addition to possibly affecting reaction on the sites, they may act to modify significantly the structure of the metal catalyst, for example by moderating metal–support interactions. Obviously, one expects that promoted catalysts prepared directly from precursors may exhibit large differences in metal dispersion. However, even when promoted catalysts are prepared from a precalcined or prereduced supported metal catalyst, the act of adding a promoter may have as much an effect in modifying the catalyst as the final presence of the promoter.

INTRODUCTION

Co-based catalysts have been demonstrated to be very effective in F–T synthesis. The high activity, the minimal formation of carbon which may increase catalyst life, the low selectivity for making CO_2, and the high selectivity for making long chain paraffins makes Co catalysts especially suitable for the indirect conversion of natural gas to liquid fuels and waxes (1–5). A review of commercial Co catalysts under development for F–T synthesis reveals that they consist typically of four major components: the primary F–T metal (Co), a second transition metal (usually noble), oxide promoters (alkali, rare earth, and/or a transition metal oxide such as ZrO_2), and a high surface area oxide support (silica, alumina, or titania) (6). The primary function of oxide promoters in general has been to improve the product selectivity. Rare earth oxides have been studied as promoters in supported catalysts such as Ni, Co, Ru, Pd, and Fe (7–21). Most of the work in this area, however, has centered around the effect of these rare earth oxides on catalyst selectivity and activity (10–16). Only a few studies have addressed the effect of these promoters on the structure of the metal catalysts (17–21).

Barrault and Guilleminot (18) observed a 100-fold increase in specific activity and TOF as a result of low levels of La addition to a Co/C catalyst. They attributed this promotional effect to the creation of new sites and not to the inhibition of carbon monoxide adsorption. Ledford *et al.* (17) investigated two methods of preparing La-promoted 10 wt% Co/Al_2O_3 catalysts. They observed promotional effects only when La^{3+} was impregnated first followed by Co and no effects when La^{3+} was impregnated second on a calcined Co/Al_2O_3 catalyst. For catalysts with low levels of La^{3+} promotion, there was little effect on the structure or on CO hydrogenation activity. On the other hand, for higher La^{3+} loadings, La–Co mixed oxides were suggested to form, metallic Co phase dispersion was shown to be enhanced, and the TOF was found to decrease. Therefore, the method of preparation and the concentration of La^{3+} appear to be important factors in obtaining promotional effects.

Recently, Co silicate has been shown to form as a result of aqueous impregnation of *reduced* and passivated Co/SiO_2 (22). In that study it was shown that water impregnation and subsequent drying had a severe effect on the structure of a reduced catalyst. The Co oxide phase declined in favor of Co silicate formation which reduced completely only above 800°C.

Ethane hydrogenolysis is a structure-sensitive reaction which has largely been utilized to study supported metal and bimetallic catalysts. Structure-sensitive reactions are useful in characterizing decoration of metal surfaces by catalyst modifiers such as poisons (23, 24) since these reactions often require a relatively large ensemble of surface metal atoms for an active site. The larger the size of the reaction ensemble, the more structure sensitive the reaction. Ethane hydrogenolysis has been reported to require

[1] To whom correspondence should be addressed.

0021-9517/96 $18.00

a large reaction ensemble on the order of 12 metal surface atoms (25, 26). Ethane hydrogenolysis has been used successfully with hydrogen chemisorption to study potassium dispersion in a series of K^+-promoted Ru/SiO_2 catalysts (24).

This paper reports on the effects of La^{3+} addition on the Co/SiO_2 structure as determined by physical (XRD), chemical (H_2 chemisorption, TPR), and reaction (ethane hydrogenolysis, SSITKA) techniques. The objectives of this study were to determine the distribution of La^{3+} and to assess its effect on metal–support interactions and on the catalytic properties of the catalysts.

EXPERIMENTATION

Catalyst Preparation

Catalyst nomenclature. In this paper, catalyst designation is given by B-LaR, where "B" refers to the calcined, reduced, and passivated 20% Co/SiO_2 *base* catalyst; "La" to La^{3+} species; and "R" to La/Co atomic percent. In this paper, *base* refers to the original calcined–reduced–passivated batch of catalyst which was used to prepare all the promoted catalysts and the unpromoted one. Following calcination La probably exists mainly in the form of La_2O_3. Upon exposure to H_2O or CO_2, it can form LaO(OH) and $La(OH)_3$ or $La_2(CO_3)_3$, respectively (27). Heating those compounds in the absence of H_2O or CO_2 cause them to revert back to La_2O_3. La species will be referred to only as "La^{3+}" in this paper.

Preparation of the Co base catalyst. The 20% Co/SiO_2 base catalyst (B) was prepared by the incipient wetness technique using an aqueous solution of $Co(NO_3)_2 \cdot 6H_2O$ (J. T. Baker Inc.) and Cab-O-Sil silica (amorphous fumed silica powder from Cabot Corp.). A 20 wt% loading was used since this would be the loading typical for a supported Co catalyst in a commercial Fischer–Tropsch synthesis process. The solution pH used was 5. Incipient wetness occurred at about 1.8 ml/g of silica. Impregnation was followed by drying at 90° overnight, calcining in flowing air at 300°C for 6 h, and reducing in flowing H_2 at 350°C for 22 h. Temperature ramp rates used during calcination and reduction were 1°C/min. The catalyst was passivated after reduction by allowing air to leak slowly into the reduction chamber at room temperature.

Preparation of La-promoted Co catalysts. Catalysts B-LaR were prepared by impregnating to incipient wetness the base catalyst B with the appropriate amounts of aqueous solutions of $La(NO_3)_3 \cdot 5H_2O$ (Aldrich Chemical Company, Inc.) to obtain catalysts with La/Co *atomic ratios* of 0.0, 0.05, 0.1, 0.2, 0.3, 0.5, and 0.75. The catalyst having La/Co = 0.0 was prepared by impregnation of the base catalyst with distilled water in order that all the catalysts would be exposed to the same procedure and conditions. This was followed by drying overnight at 90°C and rereduction in flowing H_2 at 350°C for 22 h. A La/SiO_2 catalyst (La–S), consisting of La^{3+} (equivalent in amount to that of B-La75), was also prepared for reference.

Elemental Analysis

Elemental analysis using inductively coupled plasma spectroscopy (ICP) (Galbraith Laboratories) was carried out to determine final Co loadings. ICP was also done on the water phase of a (20% Co/SiO_2 + water) slurry heated at 90°C for 12 h to investigate any leaching of contaminants from the silica to the solution during the drying step of the catalyst preparation.

XRD Measurements

X-ray measurements were performed on a Philips X'pert System X-ray diffractometer with monochromatized Cu $K\alpha$ radiation. The XRD instrument was operated at 40 kV and 30 mA. Three hundred milligrams of each catalyst was placed inside a dish for XRD. Using the same amounts for all the catalysts permitted quantitative analysis based on the XRD profiles. The spectra were scanned at a rate of 2.4°/min (in 2θ).

Static Hydrogen Chemisorption

Gas volumetric chemisorption was measured using the method of Reuel and Bartholomew (28). One gram of catalyst was first heated in 100 cc/min of H_2 to 320°C at a rate of 1.6°C/min and then held at this temperature for 12 h in order to rereduce it. H_2 was then desorbed for 1 h at 320°C under a vacuum of 10^{-6} Torr. After H_2 chemisorption for 5 h at 100°C with an initial H_2 pressure of 350 Torr, the adsorption isotherms were measured at 25°C by the decreasing pressure method. The high temperature for initial adsorption was used since the chemisorption process is known to be highly activated on cobalt (29). One hour was allowed for equilibration at each H_2 pressure at 25 °C. The amount of total chemisorption was obtained by extrapolating the total adsorption isotherm to zero pressure. The reversible H_2 desorption isotherm was measured at 25°C following evacuation of the catalyst for 10 min at that temperature. The total amount of chemisorbed H atoms was used to determine the number of vacant Co° atoms at the surface using the relationship $H/Co_s = 1$ (28).

Temperature Programmed Reduction (TPR)

TPR experiments were carried out on the Co catalysts using an Altamira Instruments AMI-1. A catalyst was reoxidized by flowing ultra pure O_2 over it while heating at a ramp rate of 5°C/min to 350°C. This temperature was maintained for 6 h to ensure complete oxidation; then the temperature was allowed to decrease to 40°C while still in O_2 flow. Ar was passed through the catalyst bed at 40°C

for 1/2 h, in order to flush the gas phase and any weakly adsorbed O_2 on the catalyst from the system, TPR was carried out using a 5% H_2 in Ar gas mixture (Matheson) as the reducing gas with a flow rate of 30 cc/min and a temperature ramp of 5°C/min to 900°C. The amount of H_2 consumed by the catalyst was measured by a thermal conductivity detector (TCD) and recorded as a function of temperature.

Ethane Hydrogenolysis

The experimental configuration for this reaction was a differentially operated, fixed-bed Pyrex reactor. A gas mixture of 10% ethane in H_2 (Linde, CP grade) was used without any further purification. Additional H_2 (Liquid Carbonic Specialty Gas Corporation, Ultra Pure) for the reaction was further purified by passing through a Deoxo unit and an activated charcoal trap. He (Liquid Carbonic Specialty Gas Corporation, Ultra Pure, 99.999%) was used as a diluent after passing through a molecular sieve trap. Brooks mass flow controllers were used to control the flow of gases. A catalyst was first heated in 100 cc/min of H_2 to 320°C at a rate of 1.6°C/min and then held at this temperature for 12 h in order to rereduce it prior to reaction. The flow rates used for reaction were $H_2/C_2H_6/He = 15/0.3/84.7$ cc/min at 101 kPa pressure. A six-way valve was used to switch between the reaction mixture and H_2 flows. Reaction temperatures and flow rates were selected to give conversions of less than 5% for catalyst samples of 35 mg.

In order to study initial reaction on a clean catalyst with minimal deposited carbon, product stream analysis was done after only 5 min of reaction. The catalyst was then bracketed with H_2 for 30 min at reaction temperature. This was shown to effectively maintain the initial activity of the catalyst. The data for the Arrhenius plots were obtained by taking the first reaction measurement at 280°C, the highest reaction temperature used in this study. The rest of the reaction data were then taken at lower temperatures in 20° intervals with hydrogen bracketing between reaction measurements. After measurement at the lowest temperature, the temperature was increased to the initial temperature of 280°C and the activity remeasured to ensure that the catalyst had not undergone any significant change. Product analysis was performed using a Perkin Elmer 8500 Gas chromatograph fitted with a porapack Q column held at 90°C and a flame ionization detector (FID).

Isotopic Transient Kinetics during Ethane Hydrogenolysis

Steady-state isotopic transient kinetic analysis (SSITKA), developed in large part by Happel (30), Bennett (31), and Biloen (32), is a powerful kinetic technique for studying catalyst surfaces under reaction conditions. By using isotopic switching and keeping the reaction environment constant during the isotopic transient, accurate measurements of the concentration of intermediates and their activities under reaction conditions are possible. This technique was performed as described in detail elsewhere (33). The reaction conditions used were flow rates of $H_2/C_2H_6/He = 6/0.15/43.85$ cc/min at 202.6 kPa pressure and a temperature of 260°C.

RESULTS

XRD

XRD of the La–S reference (La^{3+}/SiO_2) showed no diffraction lines. The XRD patterns of the reduced and passivated base and water-impregnated catalysts, B and B-La0, showed characteristic peaks corresponding to Co°, CoO, and Co_3O_4 crystallites (Fig. 1). The dominant phase was Co°. XRD profiles of B-La0 and the La^{3+}-promoted catalysts showed a decreased amount of the detectable crystalline phases Co°, CoO, and Co_3O_4 as compared with the base unimpregnated catalyst (B). The La^{3+}-promoted Co catalysts also showed no X-ray diffraction lines of La_2O_3. Recalcination was done to convert these phases into Co_3O_4 for better quantitative analysis of the Co phase. Figure 2 shows the XRD results for B, B-La0, and La^{3+}-promoted (B-La10 and B-La75 having La/Co = 0.1 and 0.75, respectively) Co catalysts after recalcination. The XRD pattern of the base catalyst (B) showed characteristic peaks corresponding to Co_3O_4 crystallites. The B-La0 catalyst exhibited a decreased amount of the detectable Co_3O_4 phase compared with the base catalyst (B). The low loading catalyst (B-La10) showed a small additional decrease in the Co_3O_4 phase while the high loading one exhibited even less.

TPR

Figure 3 gives the TPR curves for the La^{3+}-promoted and unpromoted catalysts. Table 1 presents the degrees of reduction during TPR to 900°C of the recalcined catalysts.

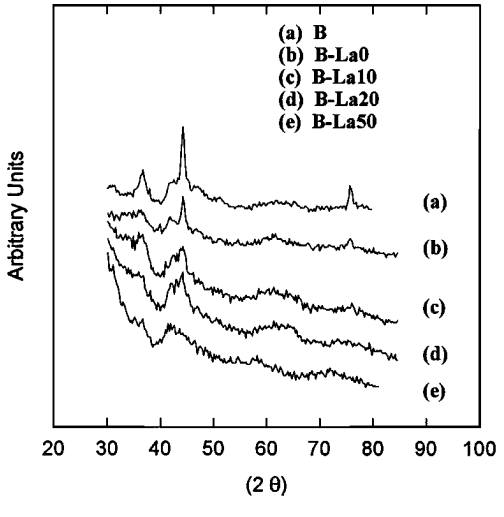

FIG. 1. XRD patterns for reduced and passivated unpromoted and La^{3+}-promoted 20% Co/SiO_2 Catalysts.

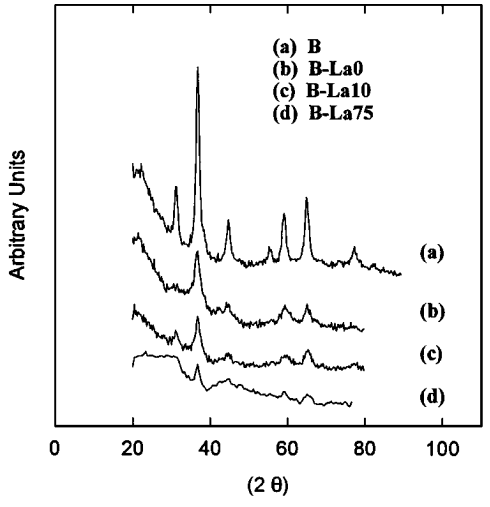

FIG. 2. XRD Patterns for unpromoted and La^{3+}-promoted 20% Co/SiO_2 catalysts after calcination at 300°C.

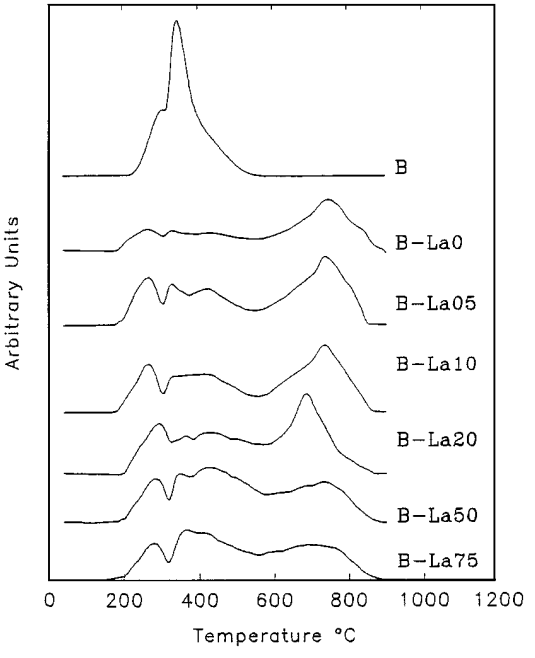

FIG. 3. Temperature programmed reduction profiles for unpromoted and La^{3+}-promoted 20% Co/SiO_2 catalysts.

The TPR profile for catalyst B in Fig. 3 shows two major reduction peaks at 280 and at 340°C and a broad shoulder extending to 500°C. The first two reduction peaks are identified to be due to Co_3O_4 which reduces in two steps (34). The broad shoulder is assigned to a Co^{3+} species interacting with the SiO_2 surface (35). For the water-impregnated catalyst (B-La0) the Co_3O_4 peaks were significantly reduced, and most of the Co was reducible only above 600°C. This high temperature species is attributed to Co silicate (34, 36). The origin of formation of this Co silicate has been discussed in detail in an earlier paper (22). The results given in that paper showed that this Co silicate is unable to be reduced during the standard reduction treatment. This Co silicate will be designated red.-Co silicate for being reducible during TPR to 900°C. All La^{3+}-promoted catalysts showed the formation of red.-Co silicate upon La^{3+} precursor solution impregnation and drying. However, for high La^{3+} loadings (La/Co $\geq$ 0.5) the amount of red.-Co silicate (reducible in the range 600–900°C) was sharply diminished.

The base catalyst (B) had a total reduction level of 80% (see Table 1). The total degrees of reduction on TPR to 900°C for the water impregnated catalyst and the La^{3+}-promoted (La/Co = 0.05, 0.1, 0.2, 0.5, and 0.75) catalysts were 70, 88, 95, 95, 80, and 67%, respectively. It is therefore noted that La^{3+} promotion of Co/SiO_2 with low La^{3+} loadings (La/Co $\leq$ 0.2) led to an improved total degree of reduction. However, for La/Co $\geq$ 0.5, the total degree of

TABLE 1

Reducibility Data for Unpromoted and La-Promoted 20% Co/SiO_2

Catalyst	% Co reduced during TPR[a] to 900°C	% Co reduced during standard reduction[b] at 320°C	Difference in reducibility (% red. at 900°C − % red. at 320°C)
B (20% Co/SiO_2)	80	80	0
B-La0	70	30	40
B-La05	88	50	38
B-La10	95	47	48
B-La20	95	50	45
B-La50	80	51	29
B-La75	67	48	19

[a] $Co_3O_4 + 4H_2 \rightarrow 3Co + 4H_2O$ for species reducing below 500°C: mol Co reduced = 3/4 (mol H_2 consumed). $CO_2SiO_4 + 2H_2 \rightarrow 2Co + SiO_2 + 2H_2O$ for species reducing from 500–900°C: mol Co reduced = mol H_2 consumed. % reduction = [(total mol Co reduced)/(total mol of Co)] × 100%. Error estimated at ±10%.

[b] Obtained from TPR 100–900°C after *in situ* reduction at 320°C for 12 h.

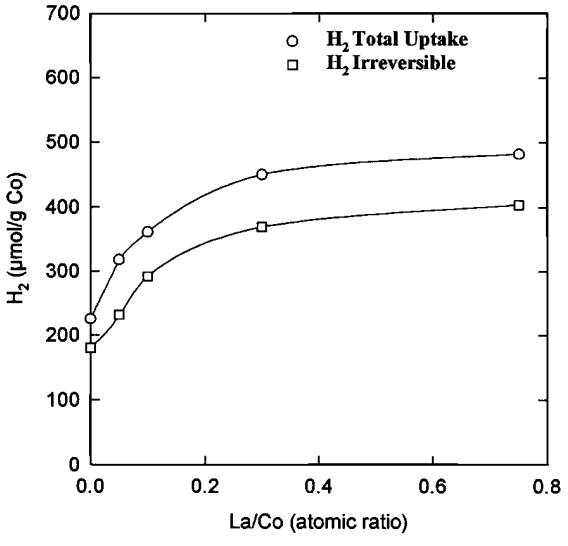

FIG. 4. Static hydrogen chemisorption uptake for La^{3+}-promoted 20% Co/SiO_2 catalysts versus La/Co atomic ratio.

reduction decreased. The results indicate the existence in all cases of a portion of the Co not able to be reduced for $T \leq 900°C$. This Co is possibly a form of Co silicate not reducible below 900°C.

Table 1 also presents the degree of reduction based on the amount of Co reduced during reduction at 320°C, estimated by digital subtraction of the TPR profile of the catalyst signal following TPR to 900°C after *in situ* rereduction at 320°C from the profile of a standard TPR of the calcined catalyst from 40 to 900°C. The degree of reduction during the standard reduction procedure (at 320°C) is more applicable for determination of the amount of Co° and its particle size for the catalysts *as normally used.* The performance of such calculations revealed reduction levels at 320°C of 80% for the base catalyst, B, 30% for the water-impregnated one (B-La0), and about 50% for all the La^{3+}-promoted catalysts. It is therefore clear that La^{3+} promotion led to improved reducibility at 320°C over the water-impregnated catalyst B-La0.

TABLE 2

H_2 Chemisorption[a] Data for Unpromoted and La-Promoted 20% Co/SiO_2 Catalysts

	μmol H_2/g cat		μmol H_2/g Co		
Catalyst	Total	Irr.	Total	Irr.	d_p[b] (nm)
B	76	59	380	295	18
B-La0	45	36	225	180	11
B-La05	51	37	318	231	13
B-La10	58	47	361	292	12
B-La30	67	55	450	369	9.5
B-La75	62	52	482	404	9

[a] Static H_2 chemisorption at 100°C. Error estimated at ±10%.

[b] Estimated assuming $H_{tot}/Co_s = 1$, 5.46×10^{-20} m^2/Co_s, $d_p = 5/S_{Co}/\rho_{Co}$, and based on % Co reduced during standard reduction at 320°C (see Table 1).

Hydrogen Chemisorption

Table 2 presents the results of static H_2 chemisorption at 100°C on the base 20%Co/SiO_2 catalyst (B), the water impregnated catalyst (B-La0), and the La^{3+}-promoted catalysts. Since the weight percentage of Co in the La^{3+}-promoted catalysts differed substantially from that in the original unpromoted catalysts (due to the weight of the La added), the hydrogen uptakes were also calculated on a per gram Co basis (see Table 2). The total H_2 uptakes for catalyst B and B-La0 were 380 and 225 μmol $H_2/g \cdot Co$, respectively. Figure 4 shows plots of the total hydrogen uptake and the irreversible uptake as a function of La^{3+} content of the impregnated Co/SiO_2. These data show that the H_2 uptake increased with La^{3+} loading up to La/Co = 0.3 (catalyst B-La30) and then leveled off for higher La^{3+} loading. The number of surface Co° atoms (estimated based on the assumption $H_{tot}/Co_s^\circ = 1$) and the percentage reduction at 320°C were used to calculate the average Co metal particle size, d_p. The average d_p of the base catalysts B and B-La0 were determined to be 18 and 11 nm, respectively. On the other hand, d_p ranged from 13 nm for B-La05 to 9 nm for B-La75. These calculations were based on the total hydrogen uptake, which has been suggested to more accurately represent Co metal dispersion on silica (28). Obviously, any blockage of the Co surface by La^{3+} would be expected to have an impact on the accurate determination of d_p based on hydrogen chemisorption.

Ethane Hydrogenolysis

Reaction was carried out on these catalysts between 220 and 280°C. Table 3 displays the ethane hydrogenolysis rates for the catalysts at 280°C, the turnover frequencies, and the apparent activation energies. The activity of the water-impregnated catalyst (B-La0) was 25% lower than that of the unimpregnated base catalyst. Figure 5 is a plot of the rate versus the La^{3+} content for the impregnated Co/SiO_2 catalysts. The following observations can be made regarding the effect of La^{3+} addition on the specific activities of these catalysts. The specific activity went through a maximum for La/Co = 0.1 (catalyst B-La10) and then decreased to a level that was still higher than that of the water-impregnated catalyst B-La0. The same trend is observed in comparing the La^{3+}-promoted catalysts with the unimpregnated base catalyst B, except that the activities for the highest La^{3+} loadings were slightly less than that of B. An examination of the activation energy with respect to La^{3+} content shows a decrease from 22 to 17 kcal/mol between the base and the highest La^{3+} loaded catalysts. However, there was really

TABLE 3

Ethane Hydrogenolysis over Unpromoted and La-Promoted 20% Co/SiO_2

Catalyst	Rate[a] (nmol/g Co/s)	TOF[b] (s^{-1}) × 10^3	E_{app}[c] (kcal/mol)
B	1785	2.4	22
B-La0	1300	2.9	21
B-La05	1835	2.9	19
B-La10	2453	3.4	22
B-La20	2297	—	21
B-La30	1985	2.2	19
B-La50	1579	—	18
B-La75	1531	1.6	17

[a] 280°C; 101 kPa; H_2/C_2H_6/He, 15/0.3/84.7 cc/min; reproducibility, ±3%.
[b] Based on total H_2 chemisorption.
[c] For reaction in the temperature range 220–280°C.

little difference in E_{app} until the highest loadings of La^{3+} (La/Co ≥ 0.5). Based on hydrogen chemisorption data, the TOF value increased for the water-impregnated catalyst and for the low La^{3+}-promoted catalysts (La/Co ≤ 0.1) and then decreased with increasing La^{3+} loading relative to the base catalyst B.

To better assess the nature of the surface activity of these catalysts, steady-state isotopic transient kinetic analysis (SSITKA) of ethane hydrogenolysis was performed. SSITKA is a powerful kinetic technique for the determination of surface concentrations of active intermediates and their specific activities under steady-state reaction conditions. The SSITKA results were evaluated based on a model developed by Chen and Goodwin using experimental measurements (33). According to this model, the reaction can

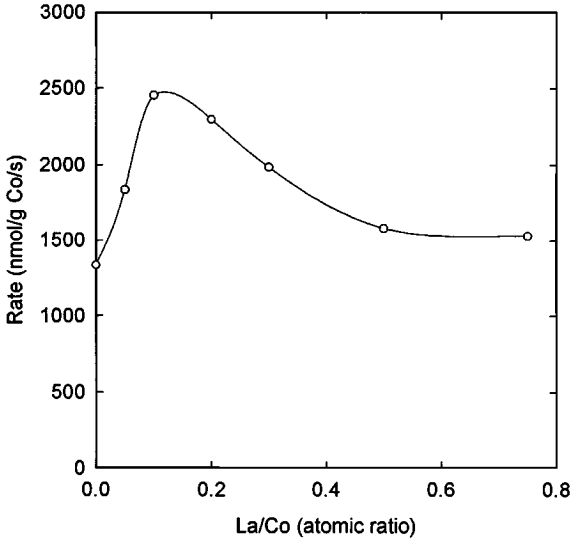

FIG. 5. Ethane hydrogenolysis rate for La^{3+}-promoted 20% Co/SiO_2 catalysts versus La/Co atomic ratio.

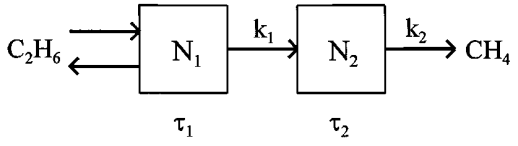

FIG. 6. Surface reaction model for ethane hydrogenolysis over the 20% Co/SiO_2 catalyst.

be considered to proceed via two pools of surface intermediates in series with the initial pool exhibiting reversible adsorption of ethane (see Figure 6). The first pool consists of intermediates, C_2H_x, and the second one consists of mono-carbon species, CH_y. This model allows for the determination based on the isotopic transients of the average residence time (τ_j) of carbon-containing species on the surface, the concentrations of intermediates in each pool (N_i), and pseudo-first-order rate constants (k_i). k_1 is a measure of the activity of C–C bond rupture, and k_2 is that of the hydrogenation step. They both, however, potentially also contain the surface concentration of chemisorbed hydrogen. Since one cannot determine the fraction of ethane which adsorbs on the active sites, $\tau_{C_2H_6,m}$ ($\tau_{C_2H_6}$ measured) is only an average value for time of surface holdup for *all ethane molecules* (some of which undoubtedly did not adsorb). Therefore, $\tau_{C_2H_6,m} \leq \tau_{C_2H_6}$ (the actual average residence time of *only adsorbing/desorbing ethane molecules*). Consequently, $\tau_1 \geq \tau_{C_2H_6,m}$ and $\tau_2 \leq (\tau_{CH4,m} - \tau_{C_2H_6,m})$. The calculation of these parameters and their relationships to their theoretical parameters, as derived and discussed in reference (33), are shown in Table 4. As seen in Table 4, values calculated for N_i's, τ_i's, and K_i's, τ_i's are estimations reflecting either maximal or minimal values. However, for comparison purposes, these estimations will be used and the parameters will be referred to by their theoretical names.

The SSITKA results (see Table 5) show that a measure of the true "TOF" of C–C bond rupture, k_1, more than doubled relative to the base catalyst (B) upon impregnation with dis-

TABLE 4

Calculation of the SSITKA Parameters and Their Relationships to the Theoretical Values

Parameter	Theoretical relationship	Relationship to measurements used to estimate parameters
N_1	N_T[a]–N_2	$\geq N_T - R_{C_2H_6} \cdot (\tau_{CH_4,m} - \tau_{C_2H_6,m})$
N_2	N_2	$\geq R_{C_2H_6} \cdot (\tau_{CH_4,m} - \tau_{C_2H_6,m})$
τ_1	$\tau_{C_2H_6}$	$\geq \tau_{C_2H_6,m}$
τ_2	$\tau_{CH_4} - \tau_{C_2H_6}$	$\leq \tau_{CH_4,m} - \tau_{C_2H_6,m}$
k_1[b]	$R_{C_2H_6}/N_1$	$\leq R_{C_2H_6}/[N_T - R_{C_2H_6} \cdot (\tau_{CH_4,m} - \tau_{C_2H_6,m})]$
k_2[b]	$1/(\tau_{CH_4} - \tau_{C_2H_6})$	$\geq 1/(\tau_{CH_4,m} - \tau_{C_2H_6,m})$

[a] N_T is based on stopping the flow of ethane and measuring the total amount of surface intermediates reacted off in H_2.
[b] Pseudo first order rate constants.

TABLE 5

SSITKA of Ethane Hydrogenolysis at 260°C

Catalyst	$R_{C_2H_6}$[a] (μmol/g Co/s)	TOF_H[b] $\times 10^3$	$\tau_{C_2H_6}$[c] (s)	τ_{CH_4}[c] (s)	τ_1 (s)	τ_2 (s)	k_1[d] (s^{-1})	k_2[d] (s^{-1})	N_1[d] (μmol/g Co)	N_2[d] (μmol/g Co)	Θ_1[b,e] $\times 10^2$	Θ_2[b,e] $\times 10^3$
B	1.95	2.3	0.8	1.4	0.8	0.64	0.16	1.5	12.5	1.3	1.64	1.7
B-La0	0.85	3.4	0.5	1.0	0.5	0.5	0.34	2.1	2.5	0.4	0.5	0.9
B-La10	1.74	2.4	0.8	1.3	0.8	0.54	0.29	1.9	6.0	0.94	0.83	1.3
B-La30	1.53	1.7	0.9	1.4	0.9	0.5	0.28	2	5.4	0.78	0.6	0.9
B-La50	1.31	1.4	0.7	1.3	0.7	0.66	0.35	1.5	3.7	0.87	—	—
B-La75	0.85	0.9	0.8	1.5	0.8	0.65	0.55	1.5	1.5	0.55	0.15	0.6

[a] At 260°C; 202.6 kPa; H_2/C_2H_6/He, 6/0.15/43.85 cc/min.

[b] Based on static hydrogen chemisorption.

[c] Time resolution, 0.1–0.2 s.

[d] k_i is intrinsic activity of intermediates based on a pseudo-first-order rate dependence and N_i is the surface abundance of intermediates in pool one or two, based on the model developed by Chen and Goodwin (33).

[e] Θ_i is the surface coverage of intermediates $= N_i$/(total adsorbed H^b).

tilled water and drying at 90°C (B-La0). However, as can be noted, the number of intermediates in pool 1 decreased from 12.3 to 2.5. This supports the TPR, XRD, and hydrogen chemisorption results that a sizable amount of the Co phase was converted into a nonactive phase upon water impregnation and drying of the base catalyst. La^{3+} addition had a pronounced effect on the number of intermediates in pool 1, N_1. This number more than doubled for the catalysts with $La/Co \leq 0.3$ compared with the water-impregnated catalyst. However, for higher loadings of La^{3+} the number of intermediates N_1 again decreased. La^{3+} addition to the Co/SiO_2 catalysts up to $La/Co \approx 0.5$ had little effect on the measure of "true" TOF of C–C bond rupture, k_1. The observed doubling of this value for these La^{3+}-promoted catalysts (see Table 4) relative to the base catalyst B is attributed to the effects of water impregnation alone. For all the catalysts, the effects on the parameters of pool 2 were essentially identical to those for pool 1 except less significant. However, the activity of the intermediates in pool 2 (for hydrogenation) decreased for $La/Co \geq 0.5$ rather than increasing.

DISCUSSION

Effect of La^{3+} Loading on Silicate Formation and Reducibility

The addition of La^{3+} resulted in a modification of the reducibility of the Co/SiO_2 catalysts. As had been shown earlier, the sequential aqueous impregnation of Co/SiO_2 resulted in the formation of Co silicates (22), primarily red.-Co silicate (reducible at ≤ 900°C). At low La^{3+} loadings ($La/Co \leq 0.2$), the amount of normally reducible (at 320°C) Co increased from 30 to about 50% as compared with the water-impregnated base catalyst (B-La0), but no significant effects were observed on the amount of red.-Co silicate formed. The same increase in reducibility at 320°C was also noted for the high La^{3+} loading catalysts ($La/Co \geq 0.5$) but here the amount of red.-Co silicate formed decreased. The 67% increase in the degree of reduction at 320°C is attributed to an effect of La^{3+} in moderating the strong Co-support interaction resulting from aqueous impregnation of prereduced Co/SiO_2. The formation of additional nonreducible Co silicate at the highest La^{3+} loadings ($La/Co = 0.5$ and 0.75) was possibly the cause for the decrease in the amount of red.-Co silicate which occurred concurrent with a decrease in the total degree of reduction for these catalysts. A pH of 12 has been found to have a big impact on reducibility of Co/SiO_2 (37). Also, for a Ni/SiO_2 system (38), Ni silicate formation was found to be favored by a pH higher than 8. The pH of the La^{3+} solutions used here was measured to be between 7 and 8.5. However, because of La^{3+} basic properties, it is possible that, during La^{3+} solution impregnation and *drying*, the actual solution pH was higher than the initial measured value and was also higher for the higher La^{3+} loading catalysts.

Another possibility is that a La–Co oxide phase was formed. Ledford *et al.* (17) studied the effect of La^{3+} loading on the properties of $Co/La/Al_2O_3$. For $La/Co \geq 0.3$ they suggested that Co_3O_4 was suppressed in favor of an amorphous dispersed La–Co mixed oxide (17). Barrault *et al.* (18) also suggested the formation of La–Co compounds for a carbon-supported La^{3+}-promoted Co catalyst based on an observed 100-fold increase in the TOF for CO hydrogenation. In both of these studies no direct evidence for the formation of La–Co compounds was found. However, although not proven, its formation can not be ruled out.

Effect of La^{3+} on Ethane Hydrogenolysis Activity

SSITKA results can shed some light on the actual effects of La^{3+} addition on the intrinsic activity of these catalysts. SSITKA of ethane hydrogenolysis performed at 260°C

showed an intrinsic C–C bond rupture rate (k_1) for the water-impregnated catalyst (B-La0) double that of the base catalyst B. This phenomenon has been discussed thoroughly in an earlier work (22). The results presented in that paper suggested that the increase in the intrinsic rate (k_1) may have been due mainly to a decrease in the reduced Co particle size *caused by water impregnation and drying*. La^{3+}-promoted catalysts showed similar intrinsic rate constants, k_1, to that of B-La0, except for the highest La^{3+} loading. However, the hydrogenation activities, k_2, of the intermediates (CH_y) did not differ significantly for all the catalysts. Thus, based on these results, it is considered that La^{3+} had little impact on the activity of Co/SiO_2 for ethane hydrogenolysis except, perhaps, for the highest La^{3+} loading.

Effect of La^{3+} Loading on Co° Dispersion

The increase in hydrogen uptake with the increase in La^{3+} loading suggests that the number of exposed Co metal surface atoms increased. This was also indicated by the increase in activity, the degree of reduction, and the numbers of intermediates, N_1 and N_2, with low La^{3+} loadings. The decrease again in the number of intermediates for the higher La^{3+} loadings is considered to be due only to increased blockage of the ethane hydrogenolysis sites (~12 Co atoms) by La^{3+}. Previous XRD results (22) indicated a decrease in the reduced Co particle size by the aqueous impregnation alone. As a consequence of the reduced particle size effect coupled with that of La^{3+} in moderating the strong Co–support interaction discussed earlier, both resulting during aqueous impregnation, a larger Co° surface can be suggested to have been produced on the Co/SiO_2 catalyst. On the other hand, an increase in the hydrogen uptake due to hydrogen spillover from the initial adsorption sites on Co to La^{3+} species on or near these adsorption sites is also possible. However, the presence of a higher Co dispersion upon La^{3+} promotion is supported by recent CO hydrogenation studies (40) on these catalysts. The results of these studies (40) show that La^{3+} addition leads to higher CO hydrogenation activity, related directly to an increase in the number of Co sites. In addition, the TOF's for ethane hydrogenolysis remained relatively constant (for a calculated ratio).

La^{3+} Dispersion on the Catalyst

The lowest level of La^{3+} loading used was sufficient to form a unit cell monolayer on the SiO_2 surface, according to calculations based on the formation of La_2O_3. The absence of a La^{3+} XRD diffraction pattern is attributed to a well dispersed La^{3+} phase, as has been suggested previously for a 10% La_2O_3/Al_2O_3 catalyst (39). The sharp increase in hydrogen uptake upon the addition of low levels of La^{3+} ($La/Co \leq 0.1$) and its approach to a constant value for higher levels suggest that the Co surface was possibly saturated with La^{3+} at relatively low La^{3+} loadings ($La/Co \geq 0.1$). La^{3+} has been found to be well dispersed in several supported systems [Co/Al_2O_3 (17) and Ni/C (19)]. Since the Co still had significant ethane hydrogenolysis activity for even the highest loadings of La^{3+}, it can be concluded that a significant fraction, perhaps even most of the La^{3+} was sitting on the SiO_2 surface.

La^{3+} Distribution on the Co Surface

Based on the results discussed above, five possibilities can be proposed to describe the potential distribution of La^{3+} over the active Co surface. The *first* possibility is that La^{3+} exists only on the SiO_2 surface and is not on or near the Co surface at all. The *second* is that La^{3+} decorates uniformly the Co metal surface. The *third* possibility situation is that La^{3+} forms island-like structures which block part of the surface Co sites but also promote other sites. The *fourth* possibility is that La^{3+} is located at the Co-SiO_2 interface. In the following discussion the comparison of the La^{3+}-promoted catalysts will be made with the water-impregnated base catalyst (B-La0) since it is more similar to the promoted catalysts, as shown by TPR, XRD, and ethane hydrogenolysis.

Possibility 1 is not likely based on the findings that La^{3+} significantly affects the reducibility, and the hydrogen uptake of the La^{3+}-promoted catalysts.

Possibility 2 can be evaluated using the ethane hydrogenolysis results. A uniform La^{3+} distribution over the Co metal surface seems unlikely since such an occurrence would be expected to lead to a significant decline in reaction rates for even low levels of promotion due to the structure sensitivity of ethane hydrogenolysis. This was not observed and in fact all promoted catalysts had higher activities than that of the H_2O impregnated base catalyst (B-La0).

Possibility 3 can be discussed in terms of the SSITKA of ethane hydrogenolysis results. From SSITKA the numbers of intermediates N_1 and N_2 first increased with La^{3+} loading up to $La/Co = 0.1$ and then decreased moderately with increasing La/Co atomic ratio to 0.75. Thus, based on these observations and considering the structure sensitivity of the reaction, it is suggested that La^{3+} blockage of the Co surface was nonuniform and also very minimal. An island-like structure coverage can be proposed to explain such behavior, where a growth of the island size would account for the noted *moderate* decrease in intermediates for the highest loadings of La^{3+}.

The fourth possibility can also be addressed using the SSITKA results for ethane hydrogenolysis. Existence of La^{3+} only at the support–metal interface cannot account for all the blockage by La^{3+} of the Co surface determined from SSITKA for the higher loadings. As the SSITKA results show, this blockage led to a decrease in N_1 from 6 to 1.5 and in N_2 from 0.94 to 0.55 mol/g Co for an increase in the La/Co atomic ratio from 0.1 to 0.75. However, the effect of La^{3+} on reducibility of the solution impregnated Co catalysts would suggest some presence of La^{3+} species at the metal–support interface.

Recent preliminary studies of CO hydrogenation (primarily methanation) on these catalysts (40) have shown that La^{3+} addition to these catalysts leads to enhanced coverage by methane intermediates and higher activity. These results suggest that the La^{3+} and Co° phases are indeed in close proximity with each other and suggest a clear promotional effect by La^{3+} of the Co sites. Thus, the results in summary would suggest that a combination of possibilities 3 and 4 perhaps best describes the arrangement of La^{3+} with Co° surface.

CONCLUSION

It is apparent from the results of this study that La^{3+} interacted with the Co metal. Aqueous impregnation led to strong Co–support interactions resulting in a decrease in the amount of active Co° (22). The presence of La^{3+} in the aqueous solution appeared to moderate the formation of strong Co–support interactions leading to better reducibility of the Co oxide phase and to a greater number of exposed Co° atoms. However, high loadings of La^{3+} ($La/Co \geq 0.5$), in addition to enhancing reducibility of Co/SiO_2, appeared to have led to higher interactions resulting in the formation of either a nonreducible Co silicate phase or a La–Co one due, perhaps, to higher pH of the impregnating solution. La^{3+} was found to be well dispersed over the Co/SiO_2 catalysts; however, it did not appear to be uniformly distributed on the Co metal surface. The results suggest that La^{3+} probably was present on the Co metal surface in an island-like structure and at the metal–support interface, as well as being dispersed on the SiO_2 surface.

While this study used only catalysts prepared from $Co(NO_3)_2$, it is unlikely that a different Co salt would have changed the effect of La^{3+} promotion seen. This is due to the fact that the supported Co precursor was calcined and reduced prior to the addition of the $La(NO_3)_3$ solution. Any differences which did result, however, would probably be more related to the differences produced in the original, unpromoted Co catalysts. An unpublished preliminary study carried out in our laboratory only found slight differences when $CoCl_2$ was used to prepare a supported Co catalyst rather than $Co(NO_3)_2$.

ACKNOWLEDGMENT

The authors thank the Department of Energy (Office of Fossil Energy) for funding this work under contract DE-AC22-92PC92108.

REFERENCES

1. Eri, S., Goodwin, J. G., Jr., Marcelin, G., and Riis, T., U.S. patent 4,801,573 (1989).
2. Eri, S., Goodwin, J. G., Jr., Marcelin, G., and Riis, T., U.S. patent 4,857,559 (1989).
3. Hoek, A., Joustra, A. H., Minderhoud, J. K., and Post, M. F., U.K. Pat. appl. GB 2 125 062 A (1983).
4. Fiato, R. A., Iglesia, E., and Soled, S. L., U.S. patent 4,794,099 (1988).
5. Beuther, H., Kibby, C. L., Kobylinski, T. P., and Pannell, R. B., U.S. Patent 4,613,624 (1986).
6. Goodwin, J. G., Jr., *Prepr. Am. Chem. Soc. Div. Petr. Chem.* **36**, 156 (1991).
7. Kazi, A., Beddu-Adou, F., and Goodwin, J. G., Jr., *Prepr. Am. Chem. Soc. Div. Petr. Chem.* **37**, 234 (1992).
8. Vada, S., Chen, B., and Goodwin, J. G., Jr., *J. Catal.* **153**, 224 (1995).
9. Oukaci, R., Goodwin J. G., Jr., Marcelin, G., Singelton, A., *Preprints of the Division of Fuel Chemistry, Am. Chem. Soc.* August 21–25 (1994).
10. Rieck, J. S., and Bell, A. T., *J. Catal.* **96**, 88 (1985).
11. Fleisch, T. H., Hicks, R. F., and Bell, A. T., *J. Catal.* **87**, 398 (1984).
12. Chen, Y. W., and Goodwin, J. G., Jr., *React. Kinet. Catal. Lett.* **26**, 453 (1984).
13. Gelthorpe, M. R., Mok, K. B., Ross, J. R. H., and Sambrook, R. M., *J. Mol. Catal.* **25**, 253 (1984).
14. Kieffer, R., Kiennemann, A., Rodriguez, M., Bernal, S., and Rodriguez-Izquierdo, J. M., *Appl. Catal.* **42**, 77 (1988).
15. Schaper, H., Doesburg, E. B. M., de Korte, P. H. M., and van Reijen, L. L., *Appl. Catal.* **14**, 371 (1985).
16. Baker, B. G., and Clark, N. J., *Stud. Surf. Sci. Catal.* **31**, 455 (1987).
17. Ledford, J. S., Houalla, M., Proctor, A., Hercules, D. M., and Petrakis, L., *J. Phys. Chem.* **93**, 6770 (1989).
18. Barrault, J., and Guilleminot, A., *Appl. Catal.* **21**, 307 (1986).
19. Barrault, J., and Chafik, A., *Appl. Catal.* **67**, 257 (1991).
20. Yermakov, Yu. I., and Ryndin, Yu. A., *in* "Proceedings, 5th Int. Symp. Relat. Homogeneous Heterog. Catal." (Yu. I. Yermakov, and V.A. Likholobov, Eds.), pp. 1019–1040. VNU Sci. Press, Utrecht, Netherlands, 1986.
21. Wang, D.-Z., Cheng, X.-P., Huang, Z.-E., Wang, X.-Z., and Peng, S.-Y., *Appl. Catal.* **77**, 109 (1991).
22. Haddad, G. J., and Goodwin, J. G., Jr., *J. Catal.* **157**, 25 (1995).
23. Martin, G. A., *Catal. Rev. Sci. Eng.* **30**, 519 (1984).
24. Hoost, T. E., and Goodwin, J. G., Jr., *J. Catal.* **130**, 283 (1991).
25. Martin, G. A., and Dalmon, J. A., *Acad. Sci. Ser. C.* **286**, 127 (1978).
26. Dalmon, J. A., and Martin, G. A., *J. Catal.* **66**, 214 (1980).
27. Gallaher, G., Goodwin, J. G., Jr., Huang, Chen-Shi, and Houalla, M., *J. Catal.* **127**, 719 (1991).
28. Reuel, R. C., and Bartholomew, C. H., *J. Catal.* **85**, 63 (1984).
29. Zowtiak, J. M., and Bartholomew, C. H., *J. Catal.* **83**, 107 (1983).
30. Happel, J., *Chem. Eng. Sci.* **33**, 1567 (1978).
31. Bennett, C. O., *Catal. Rev. Sci. Eng.* **13**, 121 (1976).
32. Biloen, P., *J. Mol. Catal.* **21**, 17 (1983).
33. Chen, B., and Goodwin, J. G., Jr., *J. Catal.* **154**, 1 (1995).
34. Iglesia, E., Soled, S. L., Fiato, R. A., and Via, G. H., *J. Catal.* **143**, 345 (1993).
35. Okamoto, Y., Nagata, K., Adachi, T., Imanaka, T., Inamura, K., and Takyu, T., *J. Phys. Chem.* **95**, 310 (1991).
36. Puskas, I., Fleisch, T. H., Hall, J. B., Meyers, B. L., and Roginski, R. T., *J. Catal.* **134**, 615 (1992).
37. Kogelbauer, A., Weber, J., and Goodwin, J. G., Jr., *Catal. Lett.* **34**, 259 (1995).
38. Claus, O., Kermarec, M., Bonneviot, L., Villain, F., and Che, M., *J. Am. Chem. Soc.* **114**, 4709 (1992).
39. Alvero, R., Bernal, A., Carrizosa, I., and Odriozola, J. A., *Inorg. Chim. Acta* **140**, 45 (1987).
40. Haddad, G. J., Chen, B., and Goodwin, J. G., Jr., *J. Catal.,* in press (1996).